

Field Tests on Instrumented H-Piles Driven into Dense Sandy Deposits

Feng Yu

*Ph.D., Assoc. Prof., School of Civil Engineering and Architecture, Zhejiang
Sci-Tech University, Hangzhou 310018, P. R. China*

E-mail: pokfulam@163.com

SYNOPSIS

Field tests on instrumented piles are critical to the development and improvement of design methods for pile foundations. This paper presents results of full-scale loading tests on two steel H-piles driven into dense sandy deposits. The test piles, with the embedded length of 39.6 m and 55.4 m, respectively, have a design capacity of 3540 kN. Both piles were heavily instrumented, driven into very stiff strata and loaded to failure. The load transfer and settlement characteristics of the piles are examined for various loading levels. The magnitude and distribution of the shaft friction of the piles are analyzed using the principles of soil mechanics.

KEYWORDS: capacity; field tests; sandy soils; piles.

INTRODUCTION

The capacity of piles driven into sand has been identified as being the area of greatest uncertainty in foundation design¹. Although various advanced methods have been developed for estimating the pile capacity, including the cavity expansion and the finite element approaches, current design procedures are largely empirical in nature. This status indicates the extreme complexity of the interaction between the pile and surrounding sand during the installation process and the need for additional research to understand the mechanisms involved.

Small-scale model tests may help build understanding of the performance of piles in sand. However, there is great concern over the scale and boundary effects in the interpretation of model test results^{2, 3}. Furthermore, there exists difficulty of realistically modeling the

dynamic driving process in the laboratory. It is widely accepted that full-scale load tests on instrumented piles can provide valuable and critical information on the real behaviour of driven piles in sand. By using the quality data of field tests, current design methods may be improved significantly⁴. Due to the impracticality of loading a full-sized pile to failure, however, the test piles in most of the field studies reported in the literature were relatively small in size and embedded at relatively shallow depths in loose or medium dense sand.

In this concise paper, key data of full-scale tests on two long steel H-piles driven into very dense sandy deposits are presented. Both of the piles were heavily instrumented and loaded to failure. We hope that the test results are helpful for a better understanding of the behaviour of driven H-piles in sand.

SITE CONDITIONS AND TEST SETUP

The two test piles, numbered as TP1 and TP2, were installed at two reclaimed sites in Hong Kong, China. The two sites have a similar stratigraphy, characterized by a vertical succession of fill, marine deposit, alluvium and decomposed granite (Fig. 1). The fill layers consist mainly of loose to medium dense, fine to coarse sand with some gravel or sandy silt. The marine deposit is composed of clayey and slightly silty, fine to medium-grained sand. The alluvium soil comprises silty fine to coarse sand with angular to subangular fine to medium gravel and occasionally with medium to coarse gravel. The completely decomposed granite (CDG) is a residual soil that is composed mainly of silty sand. The engineering property of CDG is therefore close to that of permeable silty sand⁵. The standard penetration tests (SPT) conducted at both sites indicate that the N values generally increase with depth (Fig. 1). This is considered to be reflection of the weathering of the granite.

Both of the test piles are steel H-piles having the cross-section of 305×305×223 kg/m and the design capacity of 3540 kN. The embedded lengths of TP1 and TP2 are 39.6 m and 55.4 m, respectively. Vibrating wire strain gauges were installed symmetrically along the shafts to measure the pile strain. The gauge cables were protected by PVC ducts and further covered by steel U-channels to ensure reliable measurements. More details of the instrumentation are presented by Yu⁶.

The test piles were driven by hydraulic hammers. The termination of driving was governed by the requirement of final sets, which were derived from the well-known Hiley driving formula. The ultimate pile capacity Q_u is related to the final set or point-penetration s by⁷:

$$Q_u = \frac{\eta WH}{(s + 0.5c)} \quad (1)$$

where W is the weight of hammer; H is the height of fall of the hammer; η is the efficiency of the hammer; and c is the elastic or recoverable movement of the pile and the cushioning assembly.

Given a specified pile driving machine and site condition, the final set can be estimated from Eq. (1). The value of s varies from case to case and is normally in the range of 10~20 mm in ten blows. The local practice indicates that piles driven in accordance with this requirement can usually penetrate into the soil stratum with the SPT-N value greater than 200.

Several days after the installation, the two piles were load tested using the maintained-load procedure. The piles were loaded and unloaded by steps with each increment or decrement of 0.5P (where P is the design capacity of the pile). For each step, the settlement at pile head was not allowed to be greater than 0.05 mm in 5 minutes. Generally three stages were involved in the loading tests. At the first stage the piles were loaded to 1.0P and then unloaded to zero. At the second stage the piles were re-loaded to 2.0P and the load was maintained at this level for 72 hrs before the complete release. At the final stage the piles were loaded to failure.

TEST RESULTS AND DISCUSSION

The relationship between the pile head settlement and the applied load is shown in Fig. 2 for the two piles. Fig. 3 shows the distributions of pile stresses along the pile shafts at the last loading stage. Some particulars of the applied loads and the measured settlements are given in Table 1.

During the cyclic loading process, pile TP1 rebounded significantly, as can be seen in Fig. 2. However, the changes in the pile-soil stiffness were insignificant for both piles. The recorded creep settlements during the period of 72-hr were not large for both piles; but the magnitudes of the residual settlements of the two piles were significantly different. Pile TP1 was finally loaded to 2.9P, with the residual settlement after unloading being about 41.5 mm; the maximum load carried by pile TP2 was 2.7P and the corresponding residual settlement was only 9.9 mm. The difference is considered to be mainly related to the stiffness of the soils surrounding the pile tips. Note that pile TP2, as compared to pile TP1, had a significantly larger penetration into the very stiff completely to highly decomposed granite.

As far as the pile stress is concerned, Fig. 3 indicates that for pile TP1 the change of the pile stress was slight within the upper part of the pile. That means a small shaft resistance in the upper part. In the lower part of the pile, the pile stress gradually decreased with depth, especially at higher loading levels, implying that a relatively large shaft resistance was mobilized along the lower portion of the shaft. For pile TP2, a significant mobilization of the shaft resistance was observed in the completely to highly decomposed granitic soil. The proportion between the base resistance and total capacity for TP1 was about 58.1% while for

TP2 it was 56.1%. Table 2 gives the values of the proportion between the base resistance and total capacity at various loading levels for the two piles. The base resistance tended to increase consistently with the applied load, but the amount of the increase is not large.

Based on the distribution of pile stress, the elastic shortening of the pile can be determined. The soil deformation at the pile tip can then be roughly estimated by subtracting the elastic shortening from the settlement recorded at the pile head. The relationships between the applied load and the components of the settlement in the last loading cycle are shown in Fig. 4. For both piles the deformation of the soil at the pile tip was found to increase significantly when the applied load approached the maximum value, implying that the soil beneath the pile approached failure. On the other hand, the deformation of the pile shaft displayed an approximately linear elastic relationship with the applied load.

In Fig. 5 the distributions of the shaft frictions along the piles are plotted for different loading levels. An attempt is made subsequently to use a simple procedure that is based on the principles of soil mechanics 8, 9 to predict the shaft friction. The purpose is to examine how well the shaft friction can be predicted.

Assuming a normally consolidated soil deposit for the first instance, the ultimate shaft friction f_{\max} at a given depth can be determined as

$$f_{\max} = K_c \tan \phi' \sigma_v' \approx (1 - \sin \phi') \tan \phi' \sigma_v' \quad (2)$$

where K_c , ϕ' and σ_v' are the coefficient of earth pressure, the effective friction angle and the initial effective vertical stress, respectively. Two major approximations have been introduced in Eq. (2): (a) the friction angle at the pile-soil interface is equal to the internal friction angle of the soil; and (b) K_c is equal to the coefficient of earth pressure at rest (i.e., K_0).

The strength of sand is strongly dependent on its state 10. Generally the friction angle decreases with increasing stress level. It is important to take account of this stress level dependency. A number of empirical correlations have been proposed to relate ϕ' and the effective mean normal stress, p' . For a residual soil in Japan (a decomposed granite called Masado), Yasufuku & Hyde 11 suggest the following empirical relation:

$$\tan \phi' = 1.04 \left(\frac{p'}{100} \right)^{-0.08} \quad (3)$$

where the effective mean normal stress has units of kPa.

Assuming that the CDG at the test sites in this study has similar properties with those of Masado, the relation expressed in Eq. (3) is employed. Further, the effective mean normal stress in Eq. (3) is approximately evaluated as

$$p' = \frac{1 + 2K_0}{3} \sigma_v' = \frac{3 - 2 \sin \phi'}{3} \sigma_v' \quad (4)$$

A simple procedure for evaluation of the ultimate shaft friction can then be formulated. For a given depth, an initial value of p' is assumed, and the friction angle ϕ' is then determined by using Eq. (3). A new value of p' can be derived from the current value of ϕ' by using Eq. (4) and a new friction angle is calculated. This procedure is repeated until the currently updated value of p' is close enough to the previous one.

The calculated distributions of shaft frictions are shown in Fig. 5 for two test piles. It seems that the prediction for pile TP1 is more reasonable than that for TP2. This is probably due to the fact that the soil condition for pile TP1 is closer to the assumption introduced in the simulation procedure. Note that a large part of the pile TP1 was embedded in CDG layer while more than a half part of TP2 was embedded in fill and alluvium layers whose properties may be significantly different from the CDG. An improvement of the predictions could be made by developing empirical relations between the friction angle and the stress level for specific soils rather than simply using Eq. (3). Other factors influencing the predictions include the two major approximations as mentioned before and, hence, further improvement could be made. For space limitations, more detailed discussion of the improvements is not presented here.

CONCLUSIONS

Field tests on instrumented piles are valuable for the improvement of design methods for pile foundations. This concise paper presents key data from full-scale tests on two instrumented H-piles driven into dense sandy soils. The test results showed that for both piles the base resistance carried about 60% of the overall capacity. It was also found that the shaft resistance was contributed mainly by the friction between the pile shaft and the completely or highly decomposed granite. A simple procedure that is based on the soil mechanics principles was used to predict the shaft frictions. The results indicate that a proper description of the stress-dependent strength of the soils would be critical to the accuracy of the predictions.

REFERENCES

1. RANDOLPH M. F., DOLWIN J. and BECK R. D. Design of driven piles in sand. *Géotechnique*, 1994, 44, No. 3, 427-448.
2. YANG J. Discussion of 'Shaft resistance of single vertical and batter piles driven in sand' by A. Hanna and T. Nguyen. *J. Geotech. Geoenviron. Eng.*, ASCE, 2005, 131, No. 1, 137-138.

- 3 . FELLENIUS B. H. Discussion of 'Side resistance in piles and drilled shafts' by M.W. O'Neill. *J. Geotech. Geoenviron. Eng.*, ASCE, 2002, 128, No. 5, 446-448.
- 4 . JARDINE R. J. and CHOW F. C. *New design methods for offshore piles*. Marine Technology Directorate Ltd, London, 1996, Publications MTD 96/103.
- 5 . LUMB P. The properties of decomposed granite. *Géotechnique*, 1962, 12, 226-243.
- 6 . YU F. *Behaviour of large-capacity jacked piles*. Ph.D. thesis, The University of Hong Kong, 2004.
- 7 . GEO. *Foundation design and construction*. GEO Publication No. 1/2006, Geotechnical Engineering Office, Hong Kong, 2006.
- 8 . BURLAND J. B. Shaft friction of piles in clay-a simple fundamental approach. *Ground Eng.*, 1973, 6, 30-42.
- 9 . MEYERHOF G. G. Bearing capacity and settlement of pile foundations. *Journal of the Geotechnical Engineering Division*, ASCE, 1976, 102, No. 3, 195-228.
- 10 . YANG J. and LI X. S. State-dependent strength of sands from the perspective of unified modeling. *J. Geotech. Geoenviron. Eng.*, ASCE, 2004, 130, No. 2, 186-198.
- 11 . YASUFUKU N. and HYDE A. F. L. Pile end-bearing capacity in crushable sands. *Géotechnique*, 1995, 45, No. 4, 663-676.



Table 1: Measured load-settlement particulars

	Q_{max} (kN)	Q_s (kN)	Q_b (kN)	Q_b/Q_{max}	S_{max} (mm)	S_{crp} (mm)	S_{res} (mm)
TP1	10266	4298	5968	0.581	101.5	2.3	41.5
TP2	9580	4211	5369	0.561	89.8	1.8	9.9

Notations: Q_{max} , maximum applied load; Q_s & Q_b , maximum load taken up by the shaft and base, respectively; S_{max} , maximum pile-head settlement; S_{crp} , pile-head settlement occurred during the 72-hr holding period; S_{res} , residual pile-head settlement after unloading from Q_{max} .

Table 2: Variation of base resistance with applied load

TP1	Applied load ($\times P$)	$1.0P$	$2.0P$	$2.5P$	$2.9P$
	Ratio of base resistance to applied load	0.526	0.569	0.573	0.581
TP2	Applied load ($\times P$)	$1.0P$	$2.0P$	$2.4P$	$2.7P$
	Ratio of base resistance to applied load	0.526	0.525	0.555	0.561

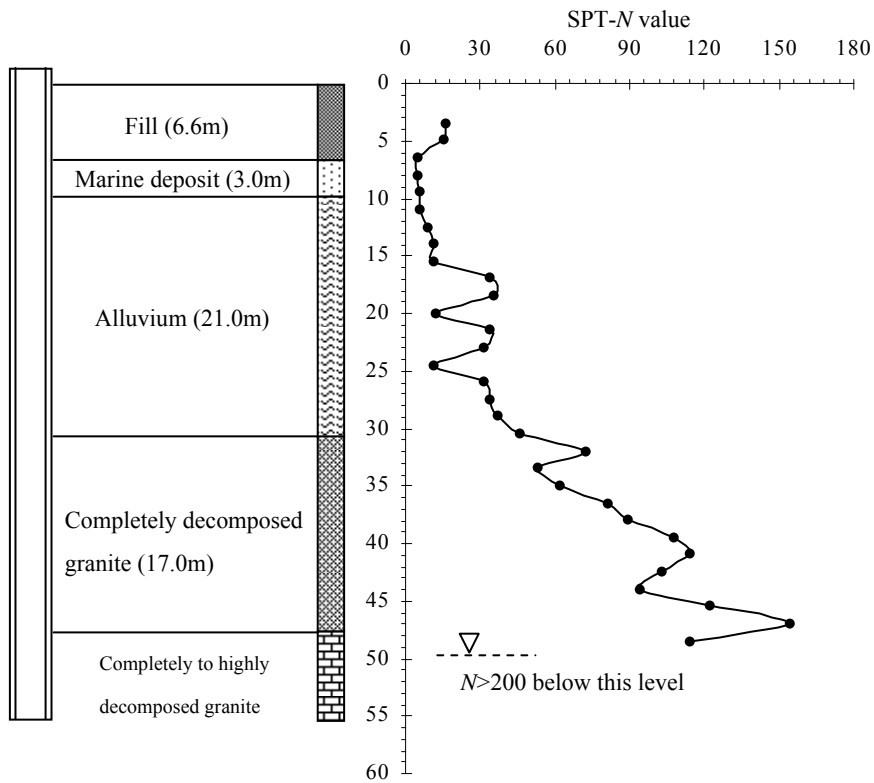
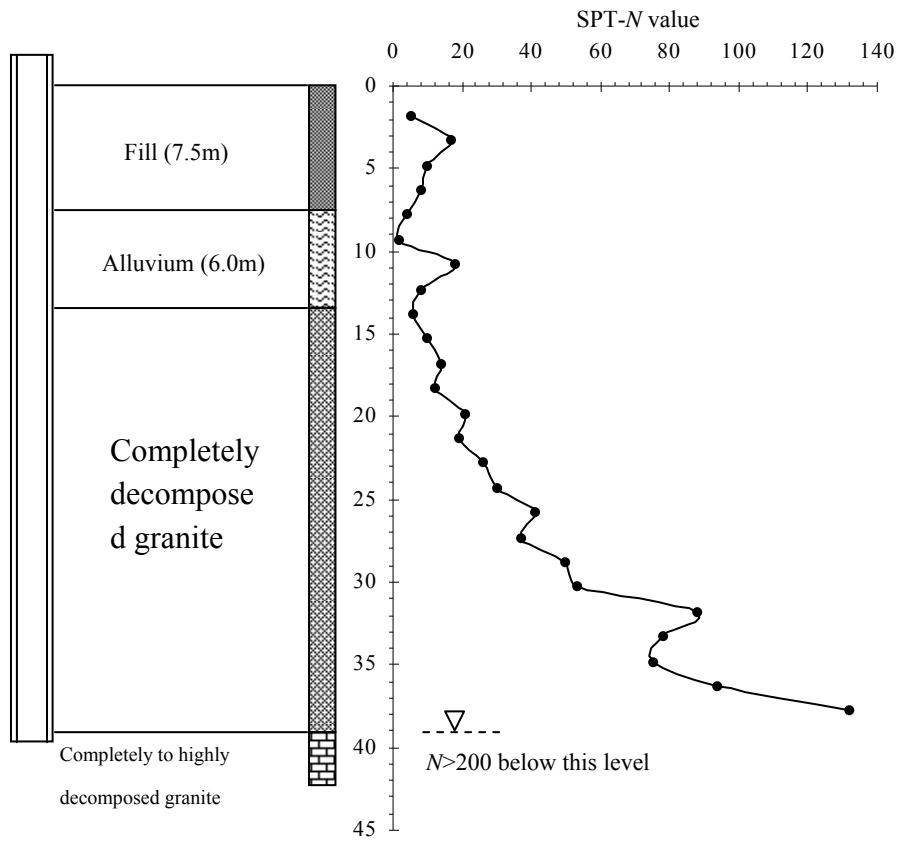


Figure 1: Soil profiles of test sites

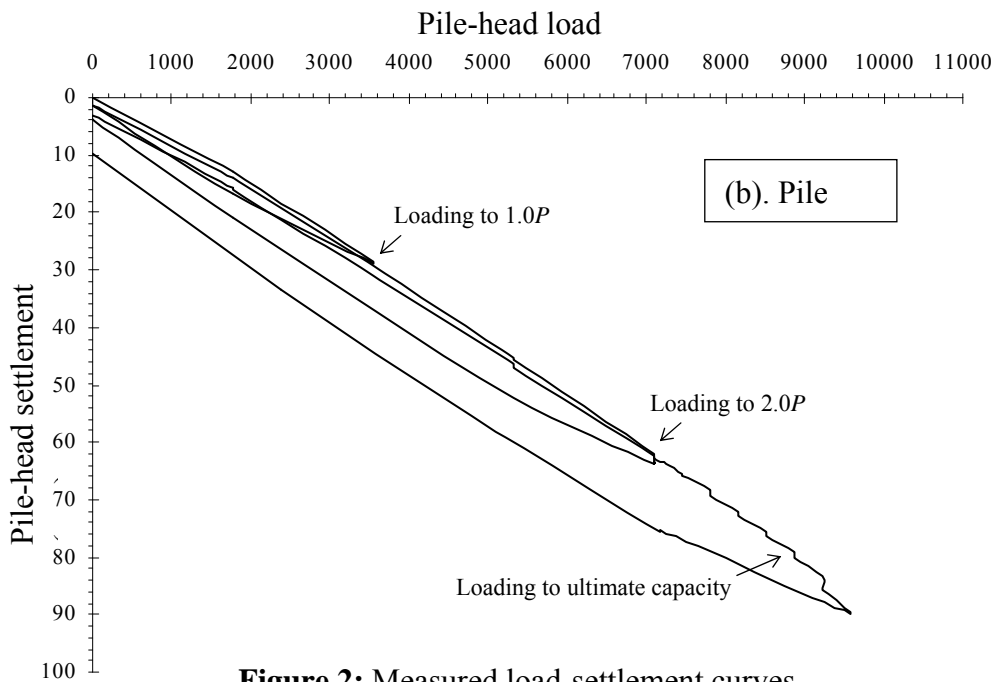
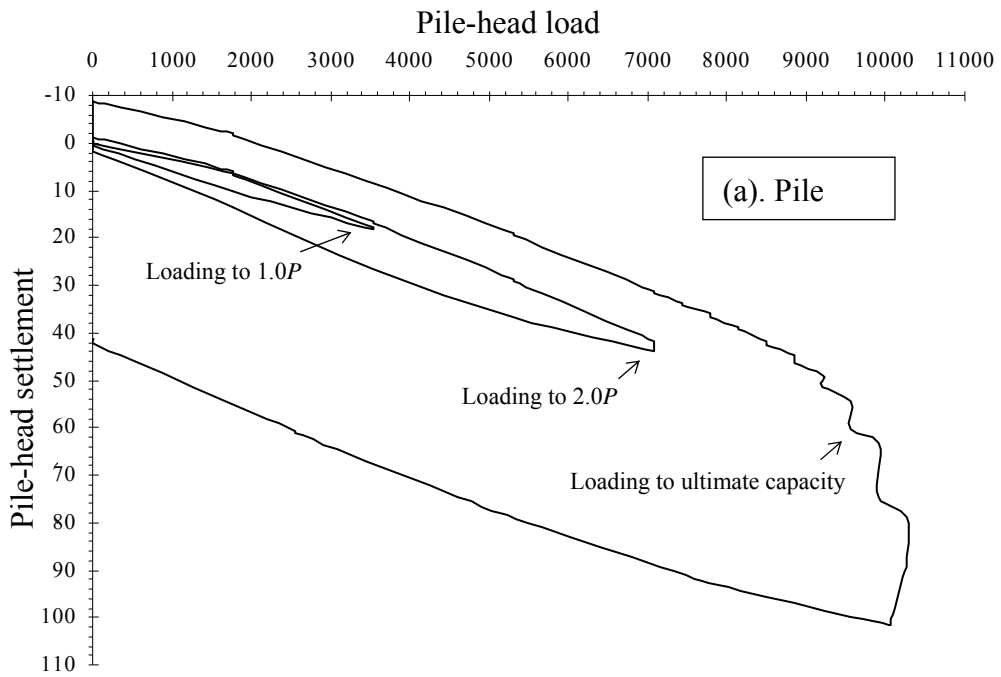
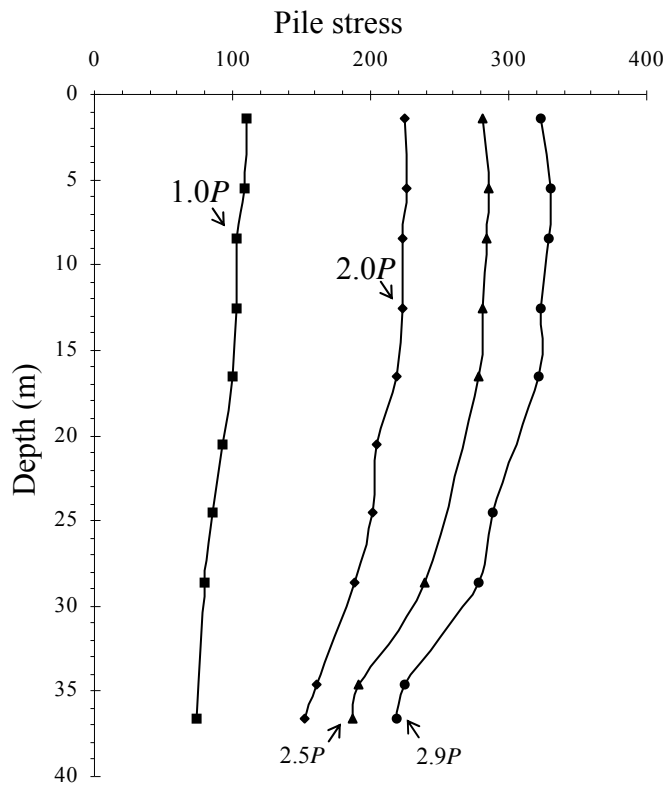
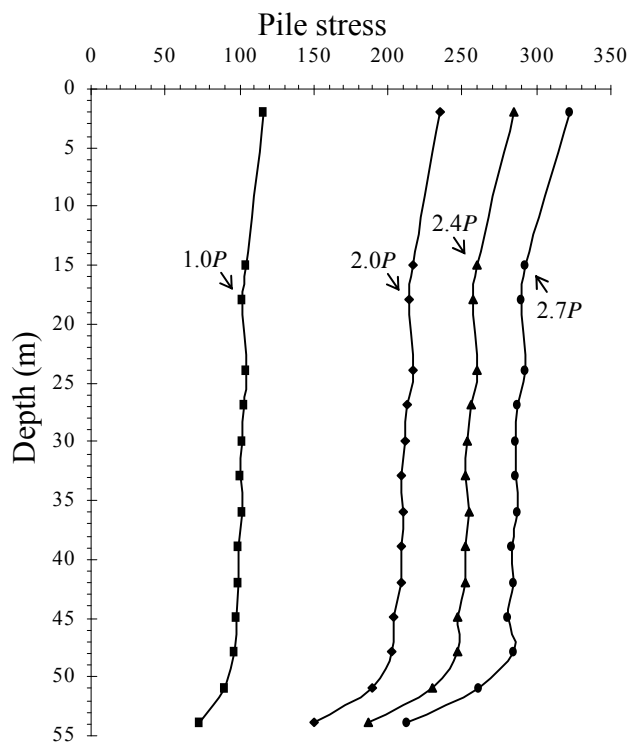


Figure 2: Measured load-settlement curves



(a) Pile



(b) Pile

Figure 3: Measured distributions of pile

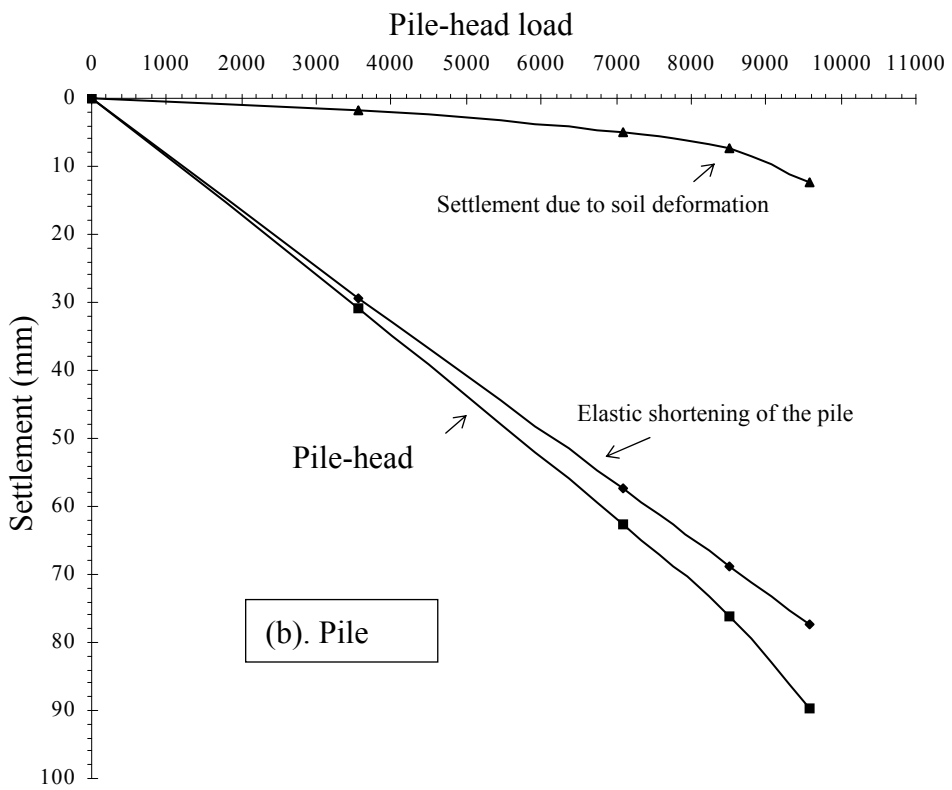
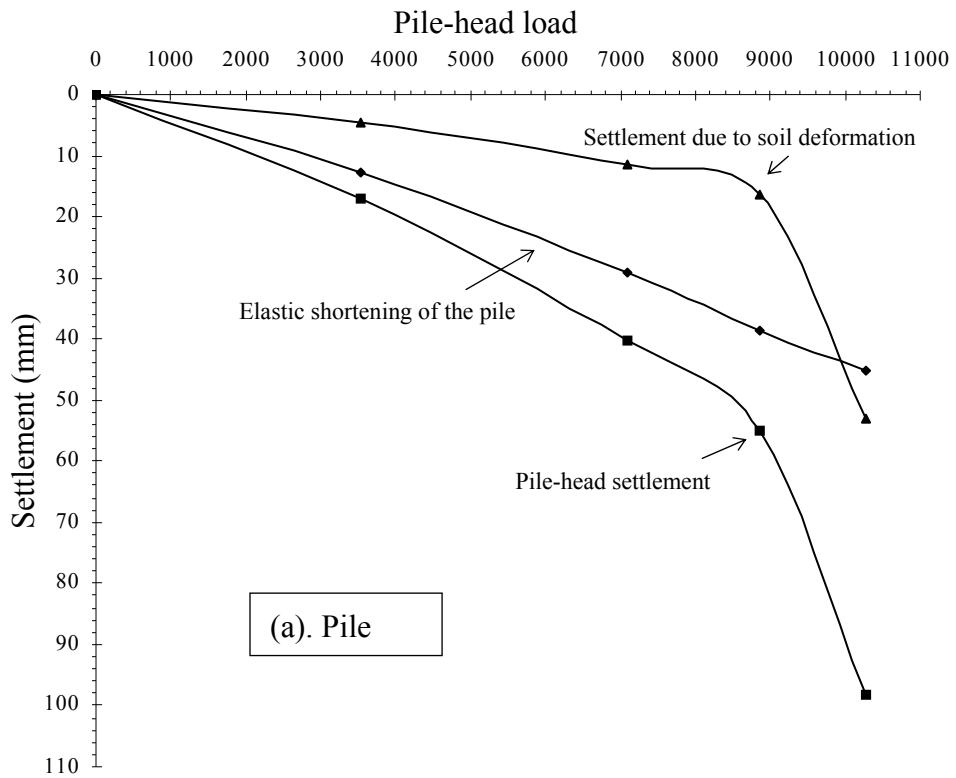


Figure 4: Relationships between load and settlement components

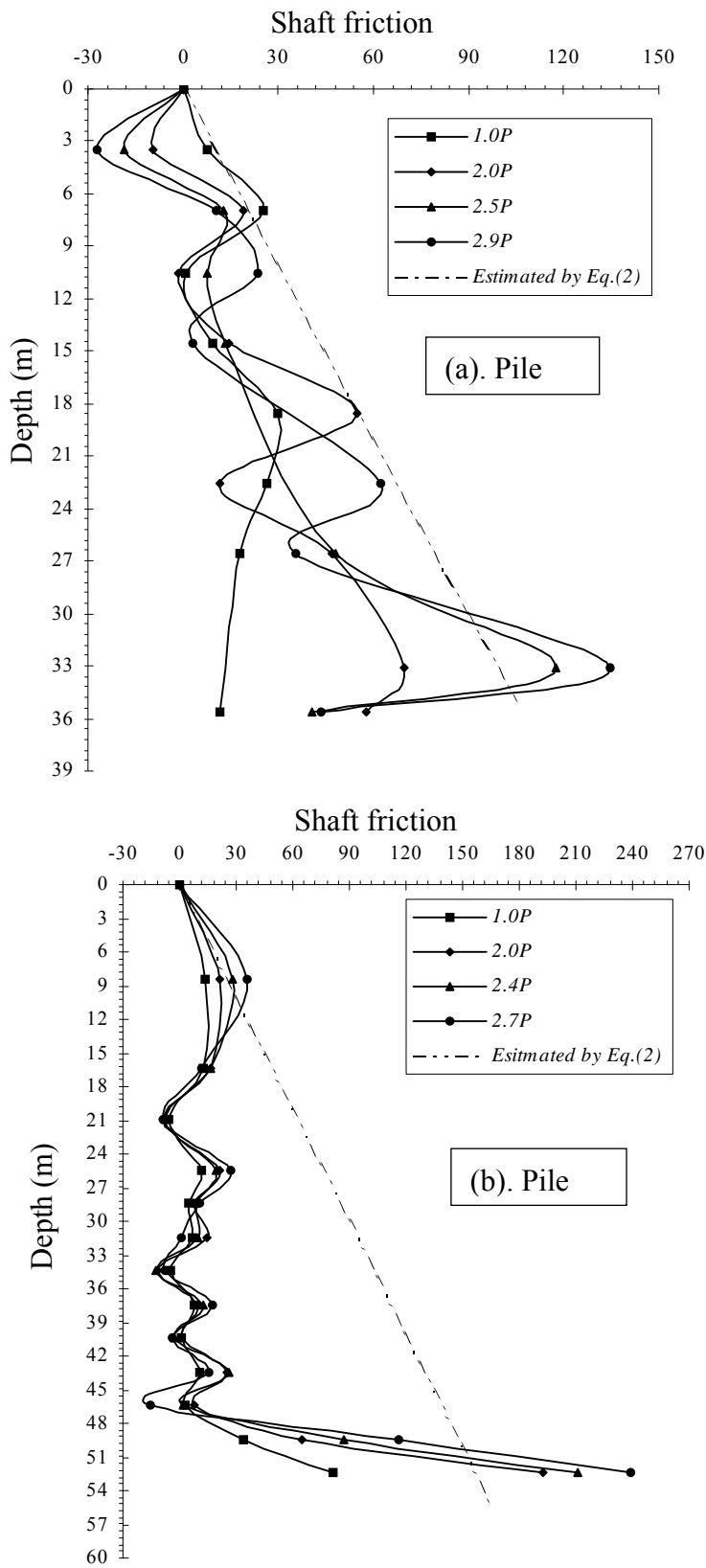


Figure 5: Measured and predicted shaft frictions